HHS Public Access

Author manuscript

J Bone Miner Res. Author manuscript; available in PMC 2021 April 01.

Published in final edited form as:

J Bone Miner Res. 2020 April ; 35(4): 714–724. doi:10.1002/jbmr.3930.

Abaloparatide at the same dose has the same effects on bone as PTH (1-34) in mice

Carole Le Henaff, Ph.D., **Florante Ricarte, Ph.D.**, **Brandon Finnie, B.S.**, **Zhiming He, M.S.**, **Joshua Johnson, M.S.**, **Johanna Warshaw, Ph.D.**, **Victoria Kolupaeva, Ph.D.**, **Nicola C. Partridge, Ph.D.***

Department of Basic Science and Craniofacial Biology, New York University College of Dentistry, New York, NY

Abstract

Abaloparatide, a novel analog of parathyroid hormone-related protein (PTHrP 1-34) became, in 2017, the second osteoanabolic therapy for the treatment of osteoporosis. This study aims to compare the effects of PTH (1-34), PTHrP (1-36), and abaloparatide on bone remodeling in male mice. Intermittent daily subcutaneous injections of 80 μg/kg/day were administered to four-month-old C57Bl/6J male mice for six weeks. During treatment, mice were followed by DEXA-Piximus to assess changes in bone mineral density (BMD) in the whole body, femur and tibia. At either four or eighteen hours after the final injection, femurs were harvested for μCT analyses and histomorphometry, sera were assayed for bone turnover marker levels, and tibiae were separated into cortical, trabecular, and bone marrow fractions for gene expression analyses. Our results showed that, compared with PTH (1-34), abaloparatide resulted in a similar increase in BMD at all sites, while no changes were seen with PTHrP (1-36). With both PTH (1-34) and abaloparatide, μCT and histomorphometry analyses revealed similar increases in bone volume associated with an increased trabecular thickness, in bone formation rate as shown by P1NP serum level and *in vivo* double labeling, and in bone resorption as shown by CTX levels and osteoclast number. Gene expression analyses of trabecular and cortical bone showed that PTH (1-34) and abaloparatide led to different actions in osteoblast differentiation and activity, with increased *Runx2*, *Col1A1*, *Alpl*, *Bsp*, *Ocn*, *Sost*, *Rankl/Opg* and *c-fos* at different time points. Abaloparatide seems to generate a faster response on osteoblastic gene expression than PTH (1-34). Taken together, abaloparatide at the same dose is as effective as PTH (1-34) as an osteoanabolic, with an increase in bone formation but also an increase in bone resorption in male mice.

Keywords

Osteoporosis; Abaloparatide; PTH; Bone; Osteoanabolics

*Corresponding Author: Nicola C. Partridge, Ph.D. New York University College of Dentistry, 345 E 24th Street, 1025B, New York, NY10010, Tel: (212) 992-7145, FAX: (212) 995-4204, ncp234@nyu.edu.

Authors' roles: Study design: CLH and NCP. Study conduct: CLH. Data collection: CLH, FR, BF, ZH, JJ, JW. Data analysis: CLH and NCP. Data interpretation: CLH, FR, BF, ZH, JJ, VK and NCP. Drafting manuscript: CLH, VK and NCP. Revising manuscript content: CLH and NCP. Approving final version of manuscript: CLH, FR, BF, ZH, JJ, JW, VK and NCP. CLH takes responsibility for the integrity of the data analysis.

Supplemental data have been included with the submission.

Introduction

Osteoporosis is a disease characterized by decreased bone mass, altered bone microarchitecture and an increase in risk of fractures (1). It is a result of a decrease in bone formation by osteoblasts, and an increase in bone resorption by osteoclasts. This imbalance between bone formation and bone resorption is due, in most cases, to a loss of estrogen, testosterone or aging. With an aging population, it is projected that there will be 6.26 million hip fractures in 2050 worldwide with a total cost of US $131.5 billion a year (2). Bisphosphonates are the most commonly used class of treatment for osteoporosis (3) but they act only on bone resorption. One important challenge is therefore to improve bone formation with an increase in osteoblast number and function in order to increase bone mass in osteoporotic bone.

Teriparatide, or PTH (1-34), was the first FDA-approved osteoanabolic therapy (4), and its effects on the skeleton remain under investigation (4, 5). Intermittent PTH (1-34) has been shown to increase bone formation to a greater extent than bone resorption in animals and humans, resulting in improved bone mass and microarchitecture (6, 7). But, after 2 years of treatment, patients present an increase in bone resorption that is thought to blunt the anabolic effect of PTH (1-34), thus creating what has been called “the anabolic window” (7-9). Nevertheless, some have argued that the PTH “anabolic window” is a misleading concept (10). Teriparatide’s anabolic effects are mediated through direct and indirect mechanisms. PTH (1-34) acts through the G-protein-coupled PTH/PTH-related peptide receptor, type 1 (PTHR1). This interaction activates several pathways including protein kinase A (PKA), protein kinase C and others that control osteoblastogenesis (6, 11, 12). The $G_{\alpha S}$/cAMP/PKA pathway is known to mediate the osteoanabolic response of PTH (1-34) (13).

In April 2017, abaloparatide, an analog of parathyroid hormone-related protein (PTHrP 1-34), was FDA-approved as a second osteoanabolic treatment. This new peptide has 41% homology to PTH (1-34) and 76% homology to PTHrP (1-34). This peptide was selected to retain stability and potent bone anabolic activity, and a low calcium-mobilization potential (14, 15). Phase III clinical trials reported that abaloparatide (at 80 μg/day) was similar, if not superior, to teriparatide (at 20 μg/day) in increasing bone mineral density in osteoporotic postmenopausal women with lower serum CTX levels, the marker for bone resorption, than in patients treated with teriparatide (16).

PTH (1-34), PTHrP (1-36), and abaloparatide all bind the same receptor, PTHR1, which is highly expressed in bone, kidney and cartilage, but also at lower levels in other tissues (11, 17). The N-terminal 34 amino acids of PTH, PTHrP and abaloparatide are sufficient for PTHR1 activation. In *in vitro* studies, PTH (1-34), PTHrP (1-36) and abaloparatide bind similarly to the G-coupled receptor (RG) whereas PTH (1-34) has a greater affinity to the non G-coupled receptor R^0 and, hence, can produce cumulatively greater signaling and biological responses than PTHrP or abaloparatide. This results in a prolonged cAMP production and is thought to cause increased bone resorption (18). Previous studies have also reported differences in downstream PTHR1 effects between PTH (1-34), PTHrP (1-36), and abaloparatide with differences in cAMP levels, PKA activation, and gene expression involved in their anabolic effects (18, 19). It has been shown that PTHrP (1-36) and

abaloparatide are weaker activators of cAMP/PKA/CREB signaling compared with PTH (1-34), as well as demonstrate a lower stimulation of *c-Fos* and *Rankl* expression in mouse osteoblasts *in vitro* and *in vivo* (19). Other studies explain that the anabolic actions of abaloparatide are due to a lower effect on resorption in rat bones and in clinical studies (20-22). However, very few studies have directly compared the effects of abaloparatide and PTH (1-34) (16, 23, 24) and only one preclinical study (25). Rather, most analyses have compared the effects of several concentrations of abaloparatide on bone in rats and in monkeys to determine the optimal dose, without comparing it with PTH (1-34) (22, 26-28). The effects of PTH (1-34) as an osteoanabolic treatment are complex and still not completely elucidated. The effect of abaloparatide, which is more similar in sequence to PTHrP (1-34), seems to have similar osteoanabolic effects as PTH (1-34). But its effects on bone remain unclear and need to be evaluated in detail. In our study, we analyzed the osteoanabolic effects of PTH (1-34), PTHrP (1-36) and abaloparatide at the same concentration, 80 μg/kg BW/day, in intact male mice.

Materials and methods

Animals

Four-month-old C57Bl/6J male mice were either purchased from Jackson Labs and/or bred in our animal facility. They were fed with a mouse standard diet (PicoLab® Rodent Diet 20, 5053, LabDiet) containing calcium (0.81%), phosphorus (0.63%) and vitamin D (2.2 IU/gm). All animals were kept in a 12 h light/dark cycle with standard rodent chow and water *ad libitum*. All animal related experimental procedures were performed in accordance with an approved protocol of the Institutional Animal Care and Use Committee of New York University. Mice (5 to 10 randomized mice per group) were injected daily, in blinded fashion, with subcutaneous human PTH (1–34) at a standard dose (80 μg/kg BW, 86% peptide content, Bachem), PTHrP (1-36, 80 μg/kg BW, 71.8% peptide content, Bachem), abaloparatide (1-34, 80 μg/kg BW, 84.1% peptide content, Bachem), or the vehicle (acetic acid, 100 μM in PBS), 5 days/week for 6 weeks. They were weighed every two weeks and followed by Dexa-Piximus to assess changes in bone mineral density (BMD) by an independent blinded person. To label bone mineralization, control and treated mice were given tetracycline (20 mg/kg, Sigma) and calcein (10 mg/kg, Sigma) by intraperitoneal injection, respectively, at days 7 and 2 before euthanasia with a lethal injection of ketamine/xylazine (7.5 mg/375 μg per animal). Two independent experiments were done: in the first experiment, the mice were euthanized 18 h after the last injection (10 animals/group) and in the second experiment, the mice were euthanized 4 h after the last injection (5-7 animals/group).

Serum Analyses

The animals were first injected with a lethal dose of ketamine/xylazine, blood samples were collected immediately by cardiac puncture, and then the animals were euthanized by cervical dislocation. The blood was allowed to clot at room temperature and sera were collected after centrifugation of blood samples at 5000 rpm for 10 minutes in order to recover the serum. Serum aliquots were frozen before ELISA analysis for the N-terminal propeptide of type 1 procollagen (P1NP) levels (Immunodiagnostic Systems Inc.) or the C-terminal crosslinking

telopeptide of type I collagen (CTX, Immunodiagnostic Systems Inc.), established markers of bone formation and bone resorption respectively. All analyses were done blinded.

Micro-Computed Tomography (μCT)

After euthanasia, femurs were dissected, cleaned of soft tissue, and stored in 70% ethanol. The samples were scanned in batches of six at a nominal resolution (pixels) of 9.7 μm using a high-resolution micro-computed tomography system (μCT, SkyScan 1172, Sky Scan, Ltd., Kartuizersweg, Kontich, Belgium). The following imaging parameters were used: 60 kV, 167 μA, and an aluminum 0.5 mm filter. All images were reconstructed using NRecon (Skyscan), a 3D morphometry evaluation program, with the following parameters: beam-hardening correction of 40, ring artifact correction of 7, and Gaussian smoothing (factor 1). The reconstructed data were binarised using a thresholding of 77–255. All three-dimensional volumetric analyses of trabecular bone and two-dimensional analyses of cortical bone were performed using the CTAn software (Skyscan). BMD of trabecular and cortical bone was determined from the binary data based on a calibration curve of calcium hydroxyapatite standards. The μCT measurements follow the guidelines reported by Bouxsein et al. (29). A 600 μm volume corresponding to 62 slices of the mid-diaphysis that began immediately distal to the third trochanter was examined for cortical bone architecture. A 1940 μm volume corresponding to 200 slices of the mid-metaphysis that began 20 slices below the growth plate was examined for trabecular bone microarchitecture. All analyses were done blinded by 2 different persons.

Histomorphometry analyses

For histomorphometry analyses, femurs were fixed in 70% ethanol, dehydrated, and embedded in methyl methacrylate (Polysciences, Warrington, PA). Longitudinal tissue sections (5 and 10 μm thick) were cut on a Leica RM2265 microtome. Histomorphometry of femurs was performed following an established protocol (30-32). Five μm thick sections were stained with Masson's trichrome to analyze structural parameters (bone volume / tissue volume (BV/TV), trabecular number (Tb.N), thickness (Tb.Th) and separation (Tb.Sp)), and with TRAP to detect osteoclasts. Unstained sections (10 μm thick) were used to assess dynamic parameters using the fluorescent calcein and tetracycline labels (mineral apposition rate (MAR), double labelled surface and bone formation rate (BFR)). BioQuant image analysis system (Nashville, TN) was used for quantitative analyses. All histomorphometry measurements were calculated and performed following the standard nomenclature approved by the American Society for Bone and Mineral Research (31, 32). All analyses were done blinded by 2 different persons.

RNA isolation and Quantitative RT-PCR Analysis

Tibiae were dissected free of soft tissues. For separation of different bone compartments, distal and proximal ends of the tibiae, corresponding to the subcortical trabecular rich region and the growth plate was first dissected. Following this, bone marrow was completely removed by centrifuging the bone and collecting the bone marrow in a new Eppendorf tube. The remaining cortical bone contained predominantly osteocytes. We extracted total RNA using a TRIzol kit (Sigma). cDNA was synthesized from 1 μg of total RNA using TaqMan® Reverse Transcription Reagents (Life Technologies, Inc.). SYBR® Green Master Mix was

used for quantitative real-time RT-PCR using a Mastercycler® realplex^2 instrument (Eppendorf). mRNA expression was calculated using the following formula $2^{\wedge\text{-}(\Delta\Delta Ct)}$. The levels of mRNA expression were normalized to geometrical means with *Gapdh* and *Hprt* expression as internal controls and then expressed as fold values compared with the vehicle-treated mice. The qRT-PCR primers are listed in Table 1. All qPCR shown were done on trabecular-rich or cortical-rich regions.

Statistical analysis

Values are presented as the means ± S.D., and shown as individual values whenever possible. Data were analyzed for normal distribution by Kolmogorov-Smimov and Shapiro-Wilk tests and "Normal Q-Q Plot" graphs. If normal distribution was not achieved, we used rank transformation and confirmed the normality by the previous tests. The equality of variance was determined with Levene's test. If both normal distribution and equality of variance were demonstrated we used one way ANOVA and Tukey's multiple comparison test or two way ANOVA or RMANOVA and Bonferroni's multiple comparison test using SigmaStat software (SPSS Sciences, Chicago IL) and GraphPad Prism 8 (2019 GraphPad Software, Inc., La Jolla, CA, USA). If we could not perform a parametric test, we used a non-parametric test such as the Kruskal-Wallis test. Because the use of p values has been recently questioned (33), we show exact *p* values in most figures as well as a Table of Effect sizes (Supplementary Tables 2 and 3). *p* values in Figures 1B-D are shown in colors corresponding to either PTH (1-34) or abaloparatide treatment for the reader's benefit.

Results

PTH (1-34) and abaloparatide similarly improved bone mineral density in mice, whereas PTHrP had no effect.

For all experiments, we used wild type male mice in order to avoid any hormone variation that occurs with female mice. In addition, adult female C57Bl/6 mice have very low trabecular bone volume and high variability compared with male mice (30, 34). We have added exact p values to most of the figures and provided Tables of Effect sizes (Supplementary Tables 2 and 3). This now allows the reader to evaluate mean differences in terms of importance as well as statistical rarity. Results continue to indicate large mean differences between control groups and groups treated with PTH (1-34) or abaloparatide, and few differences between those active treatment groups.

During the treatments, we followed mice by body weight and Dexa-Piximus, every 2 weeks, to assess changes in bone mineral density. All mice had the same range of body weight (data not shown) and body length at baseline as during the treatments (Figure 1A). PTHrP (1-36), at 80 μg/kg BW/day, had no effect on bone mineral density (BMD) at any site (whole body, femur or tibia). In contrast, PTH (1-34) and abaloparatide similarly improved BMD of tibiae, compared with the PBS controls, beginning at the 4th week of treatment (Figure 1D), with effects that were apparent in the whole body and the femur at the end of the treatment (Figure 1B and C). Abaloparatide and PTH (1-34) showed some increases during the time course, with abaloparatide showing a greater increase between 4 and 6 weeks in tibiae. All

these results were done with one experiment but they were confirmed with the second experiment.

PTH (1-34) and abaloparatide had similar stimulatory effects on trabecular bone volume, bone formation and bone cortical thickness in mice.

After euthanasia, femurs were fixed in 70% ethanol and analyzed, first, by μCT to assess bone microarchitecture and then by histomorphometry to assess osteoblast and osteoclast activity. With cortical bone, PTH (1-34, p=0.060) and abaloparatide (p=0.020) increased cortical thickness (Figure 2C) which was supported by the respective effect sizes (1.52 and 2.00, Supplemental Table 2) but without any changes in cortical bone mineral density (Figure 2B). Dynamic histomorphometry showed no changes in cortical mineral apposition rate (Figure 3F), mineralized surface (Figure 3G), or bone formation rate (Figure 3H), calculated by double labeling.

In trabecular bone, abaloparatide and PTH (1-34) both similarly increased trabecular bone with a similar increase in trabecular bone mineral density (Figure 2D), trabecular bone volume (Figure 2E), and trabecular thickness (Figure 2F). The peptides did not affect trabecular number (Figure 2G) or separation (Figure 2H). These results were confirmed by histomorphometry (Figure 2J-M) with a stronger effect for abaloparatide on trabecular thickness and number. Only PTH (1-34) had an increase in degree of anisotropy (Figure 2I) revealing better connectivity between trabeculae. These changes were reflected in an increase in trabecular bone formation shown by double labeling (Figure 3B). Both PTH (1-34) and abaloparatide treatments generated a similar increase in mineral apposition rate (Figure 3C). There was a closely similar increased bone formation rate elicited by both peptides (Figure 3E). Both treatments had mostly little effect on lumbar vertebrae trabecular bone except for abaloparatide causing an increase in trabecular thickness compared with PTH (1-34) (Supplementary Figure 1).

Accompanied by the increased bone formation rate, PTH (1-34) and abaloparatide both increased serum P1NP levels (Figure 3A), although abaloparatide gave a greater increase 18 h after the last injection.

PTH (1-34) and abaloparatide differentially regulate osteoblastic gene expression.

To confirm the action of both peptides on osteoblasts we measured osteoblastic gene expression (Figure 4). PTH has been shown to stimulate many genes involved in bone formation such as: the osteoblast-specific runt related transcription factor 2 (*Runx2*), alkaline phosphatase (*Alpl*), collagen type I alpha 1 (*Col1A1*) and osteocalcin (*Ocn*) (35, 36). We observed some differences with abaloparatide on these osteoblastic genes compared with PTH (1-34).

In trabecular bone, *Runx2*, *Alpl*, *Ocn* and *Bsp* expression were increased 4 h after the last abaloparatide injection and then decreased by 18 h. PTH (1-34) stimulated *Alpl* and *Ocn* but only at 18 h, suggesting a later effect for PTH (1-34). For *Col1A1* and *Bsp* expression, both PTH (1-34) and abaloparatide had stimulatory effects at both time points.

In cortical bone, the effects of PTH (1-34) and abaloparatide were slightly different than in trabecular bone. Only abaloparatide increased *Runx2* (at 4 h). Both PTH (1-34) and abaloparatide increased *Col1A1*, *Alpl* and *Bsp* expression at 4 h while abaloparatide increased all three of these at 18 h, with a greater effect of abaloparatide on *Col1A1* and *Alpl* at this time point. Neither had any effect on *Ocn*.

With respect to *Sost* mRNA levels, there appeared to be a different effect of PTH (1-34) at 4 h compared with abaloparatide [examining p values and effect sizes (Supplemental Table 3)].

PTH (1-34) and abaloparatide both increased bone resorption.

Serum CTX analyses demonstrated an increase in serum CTX levels that indicate an increase in bone resorption with both PTH (1-34) and abaloparatide treatments (Figure 5A). The increase in bone resorption was confirmed by histomorphometry which showed a similar increase in osteoclast number in trabecular bone (Figure 5B) with both peptide treatments. No changes were observed in cortical bone (Figure 5C).

One of the major pathways utilized in PTH-induced resorption is the receptor activator of the nuclear factor kappa B ligand (*Rankl*)/*Rank*/osteoprotegerin (*Opg*) system. It has been shown that PTH (1-34) increases osteoclastogenesis by increasing *Rankl* expression (37) and decreasing expression of *Opg*, a decoy receptor for RANKL (38). In our data, only abaloparatide rapidly increased the *Rankl*/*Opg* ratio at 4 h after the last injection, (Figure 5D and G) in trabecular bone, showing a quicker effect of abaloparatide on expression of these genes. Both PTH (1-34) and abaloparatide increased the *Rankl*/*Opg* ratio at 18 h after the last injection.

Previous reports showed that PTH (1-34) modulates the complex secondary response in the expression of matrix metalloproteinase 13 (*Mmp13*), one of the enzymes responsible for extracellular matrix degradation (39, 40). Here, both PTH (1-34) and abaloparatide elicited an increase in *Mmp13* expression in trabecular and cortical bone, 4 h after the last peptide injection which was sustained at 18 h in trabecular bone. In cortical bone, *Mmp13* stimulation decreased at 18 h after the last injection with both peptides but remained elevated with abaloparatide (Figure 5E and H).

We have shown that c-Fos is an immediate early downstream PTH effector in osteoblasts by way of cAMP/PKA signaling, and that PTH (1-34) induces a rapid increase in *c-fos* mRNA expression (19, 41). In our mouse model, only abaloparatide caused an increase in *c-fos* expression in trabecular bone 4 h after the last injection. This was followed by a slight decrease at 18 h in trabecular bone and a substantial decrease in cortical bone. PTH (1-34) affected *c-fos* expression at both 4 and 18 h in cortical bone (Figure 5F and I).

Discussion

Previous work of ours with mouse osteoblasts *in vitro* (19) has shown that PTHrP (1-36) and abaloparatide are weaker stimulators of cAMP/PKA/CRTC (CREB-regulated transcription coactivator) signaling compared with PTH (1-34). This resulted in lesser stimulation of

Rankl mRNA. In order to determine if a similar differential effect on bone occurred *in vivo*, we have conducted a head-to-head comparison of PTH (1-34), PTHrP (1-36) and abaloparatide at the same dose, 80 μg/kg BW/day, in wild type male mice. Our hypothesis from the *in vitro* data was that there would be a differential effect on bone with PTH having a greater effect than PTHrP and abaloparatide. In fact, we found that PTHrP (1-36) had no effects on bone mineral density while PTH (1-34) and abaloparatide elicited very similar increases in bone mineral density, bone volume, bone formation, and, importantly, on bone resorption.

PTHrP (1-36) had no effect on bone mineral density but had a small effect on bone formation, although no changes in bone volume were observed (data not shown). PTHrP N-terminal residues 1-13 exhibit high homology with PTH (1-34), and are thought to account for the ability of PTHrP to mimic the effects of PTH (1-34) (11). Unlike PTH (1-34), PTHrP is produced and acts locally in cartilage to promote chondrocyte proliferation and to block the cells' maturation into hypertrophic chondrocytes (42, 43). Because of its similarity with PTH, it was postulated that PTHrP (1-36) could serve as a putative osteoanabolic treatment. Some clinical studies have shown that PTHrP (1-36) results in the same increase in bone formation as PTH (1-34). However, for that to occur, PTHrP (1-36) had to be given at a 20 times higher dose (500-750 μg/day) than PTH (1-34). Surprisingly, in contrast with PTH, PTHrP (1-36)-treated patients showed no changes in bone resorption, but showed hypercalcemia (44). Compared with PTH (1-34), PTHrP (1-36) is rapidly degraded after injection and shows less volume of distribution (45). In our model, we used the same dose for all three peptides, but this dose may not be sufficient to produce the expected PTHrP anabolic effects in mice. PTHrP is known to be a cause of loss of bone with lactation (46), since it is produced by the breast and circulating concentrations are elevated. We assume that these concentrations were not produced by the daily injections of PTHrP, and in any case, the loss of bone with lactation is likely due to constantly elevated PTHrP, which is not the situation with the intermittent injections used in the present study.

Abaloparatide is an analog of PTHrP (1-34), and is identical to PTHrP at amino acid residues 1-22, but with multiple substitutions between amino acids 23-34 (38% homology). These changes maximize abaloparatide's stability compared with both PTH (which has lower homology to abaloparatide) and PTHrP (14, 24). *In vivo*, the increased stability of abaloparatide could be responsible for its prolonged action on PTHR1, and could lead to the same effect on osteoblast/osteoclast activity as PTH (1-34). The similar effect of abaloparatide and PTH (1-34) on bone formation and resorption is surprising, and is not completely in line with the pre-clinical and clinical findings (16, 20, 22, 27). One should keep in mind that in our model, unlike previous studies, we used the same dose in wild type adult male mice to assess the effect of all three peptides systematically. Data in other animal models indicate a near absence of bone resorption with several doses of abaloparatide. For example, in ovariectomized rats, abaloparatide at 25 μg/kg showed no effect on bone resorption (22). In the phase III clinical trial, the effect on bone resorption was less when post-menopausal women were treated with 80 μg/day of abaloparatide than with 20 μg/day of PTH (1-34), as monitored by plasma CTX (16). The only pre-clinical study to compare the metabolic effects of PTH (1-34) and abaloparatide *in vivo* (25) showed a similar stimulation of L4-L5 BMD and strength, and P1NP levels in ovariectomized rats treated for

4 weeks. The authors noted that they had poor effectiveness of the two peptides on the bone resorption marker, urinary DPD/Cr, *in vivo*. In fact, it is notable that levels of this marker were elevated about 3-fold in the ovariectomized rats compared with the sham-operated rats, which may have masked any effect of the two peptides on resorption, although their highest dose showed a tendency to an increase. We, on the other hand, have thoroughly investigated the effects of the two peptides systemically in intact male mice; with serum levels of P1NP and CTX and whole body BMD, and in long bones (i.e., both trabecular and cortical bone) determining BMD and bone parameters by uCT and histomorphometry as well as gene expression changes. We have observed effects on most parameters by both peptides, and probably most importantly, have seen closely similar increases in CTX levels and osteoclast number in femoral trabecular bone.

PTH (1-34) activates osteoclast differentiation and promotes bone resorption (19, 37, 47) through its action on *Rankl* expression by osteoblasts and osteocytes. We showed that PTH (1-34) upregulated the *Rankl/Opg* ratio only at 18 h after the last injection, whereas abaloparatide had a faster effect and increased the *Rankl/Opg* ratio starting 4 h after the injection. An increase in *Opg* (RANKL receptor decoy) leads to a decrease in osteoclastogenesis. In trabecular bone, *Opg* expression was not affected by the peptide treatment unlike *Rankl* expression (data not shown). In this situation, *Rankl*/*Opg* ratio reflected the *Rankl* expression and osteoclast differentiation. Faster action of abaloparatide is likely caused by a pulsatile cAMP induced by abaloparatide binding to PTHR1. *In vitro*, we showed that PTH (1-34) stimulates *Rankl* expression in primary osteoblastic cells with greater strength than PTHrP (1-36) and abaloparatide. The maximal effects of PTHrP and abaloparatide were at 2 h while PTH kept on increasing to 4 h (19). This discrepancy between the *in vitro* and *in vivo* results is possibly caused by the different peptide concentrations, time of treatment and pharmacokinetics. The amount of each peptide that reaches bone cells in animals remains unknown. *In vitro*, at 10^{-9} M, PTH (1-34) shows a greater increase in *Rankl* expression at 4 h than PTHrP (1-36) and abaloparatide, whereas at a higher concentration (10^{-8} M), *Rankl* mRNA is regulated similarly by all 3 peptides (19).

One of the major anabolic effects of PTH (1-34) *in vivo* and *in vitro* is inhibition of sclerostin (*Sost*) expression, a glycoprotein secreted by late osteoblasts and osteocytes (19, 48, 49). The main function of sclerostin is to inhibit bone formation through inhibition of the canonical Wnt/β-catenin pathway (50, 51). There appeared to be a difference in the effect of PTH (1-34) and abaloparatide on *Sost* expression However, perhaps the time points were not optimal. Alternatively, abaloparatide does not cause an anabolic effect through inhibition of *Sost*.

In most studies, abaloparatide was given to postmenopausal women with osteoporosis (16, 23, 24, 52), to ovariectomized rats (20, 22, 25), to orchiectomized rats (28) or to ovariectomized monkeys (27). In these models, the basal bone resorption level is very high because of the loss of gonadal hormones, and this could partially obscure the effect of abaloparatide on bone resorption. This could explain why we observed a stronger effect of abaloparatide on bone resorption in our model, as compared with previous studies. Also, the effects of abaloparatide might be due to an “overfilling” of BMUs, as with intermittent PTH (1-34). Indeed, the anabolic effects observed with intermittent PTH (1-34) are due to the

increased resorbed spaces of BMUs, but its effects on the osteoblast result in a net positive balance (8, 53).

In summary, abaloparatide is as effective as PTH (1-34) as an osteoanabolic agent on bone formation. Most notably, abaloparatide also has the same effects on bone resorption in intact male mice. Nevertheless, the expected superior positive outcome on bone remodeling is not achieved with the same dose of abaloparatide. Clearly, more efforts are needed in the future to develop better anabolic treatments for osteoporosis.

Supplementary Material

Refer to Web version on PubMed Central for supplementary material.

Acknowledgements

We would like to thank Gozde Yildirim and the μCT core (NIH grant, S10 OD010751 to NCP) and Bing Liu of the histomorphometry core. We are also grateful to Dr. Malvin Janal for advice on the statistical analyses. This work was supported by NIH grants 5R01 DK47420-24A1 and DK47420-24A1S1 (to NCP) and R01 AR063128-05A1 (to VK).

This work was supported by NIH grants 5R01 DK47420-24A1, DK47420-24A1S1 and S10 OD010751 (to N.C.P.) and by R01 AR063128-05A1 (to V.K.). The authors have no conflict of interest.

References

1. Liu J, Curtis EM, Cooper C, Harvey NC. State of the art in osteoporosis risk assessment and treatment. J Endocrinol Invest. 2019.
2. Harvey N, Dennison E, Cooper C. Osteoporosis: impact on health and economics. Nat Rev Rheumatol. 2010;6(2):99–105. [PubMed: 20125177]
3. Pazianas M, Abrahamsen B. Osteoporosis treatment: bisphosphonates reign to continue for a few more years, at least? Ann N Y Acad Sci. 2016;1376(1):5–13. [PubMed: 27525578]
4. Rosen CJ, Bilezikian JP. Clinical review 123: Anabolic therapy for osteoporosis. J Clin Endocrinol Metab. 2001;86(3):957–64. [PubMed: 11238469]
5. Baron R, Hesse E. Update on bone anabolics in osteoporosis treatment: rationale, current status, and perspectives. J Clin Endocrinol Metab. 2012;97(2):311–25. [PubMed: 22238383]
6. Jilka RL. Molecular and cellular mechanisms of the anabolic effect of intermittent PTH. Bone. 2007;40(6):1434–46. [PubMed: 17517365]
7. Canalis E, Giustina A, Bilezikian JP. Mechanisms of anabolic therapies for osteoporosis. N Engl J Med. 2007;357(9):905–16. [PubMed: 17761594]
8. Dempster DW, Cosman F, Kurland ES, Zhou H, Nieves J, Woelfert L, et al. Effects of daily treatment with parathyroid hormone on bone microarchitecture and turnover in patients with osteoporosis: a paired biopsy study. J Bone Miner Res. 2001;16(10):1846–53. [PubMed: 11585349]
9. Finkelstein JS, Wyland JJ, Leder BZ, Burnett-Bowie SM, Lee H, Juppner H, et al. Effects of teriparatide retreatment in osteoporotic men and women. J Clin Endocrinol Metab. 2009;94(7):2495–501. [PubMed: 19401368]
10. Seeman E, Martin TJ. Co-administration of antiresorptive and anabolic agents: a missed opportunity. J Bone Miner Res. 2015;30(5):753–64. [PubMed: 25736531]
11. Cheloha RW, Gellman SH, Vilardaga JP, Gardella TJ. PTH receptor-1 signalling-mechanistic insights and therapeutic prospects. Nat Rev Endocrinol. 2015;11(12):712–24. [PubMed: 26303600]
12. Yavropoulou MP, Michopoulos A, Yovos JG. PTH and PTHR1 in osteocytes. New insights into old partners. Hormones (Athens). 2017;16(2):150–60.

13. Li X, Liu H, Qin L, Tamasi J, Bergenstock M, Shapses S, et al. Determination of dual effects of parathyroid hormone on skeletal gene expression in vivo by microarray and network analysis. J Biol Chem. 2007;282(45):33086–97. [PubMed: 17690103]

14. Tella SH, Kommalapati A, Correa R. Profile of Abaloparatide and Its Potential in the Treatment of Postmenopausal Osteoporosis. Cureus. 2017;9(5):e1300. [PubMed: 28680788]

15. Bone HG, Cosman F, Miller PD, Williams GC, Hattersley G, Hu MY, et al. ACTIVExtend: 24 Months of Alendronate After 18 Months of Abaloparatide or Placebo for Postmenopausal Osteoporosis. J Clin Endocrinol Metab. 2018;103(8):2949–57. [PubMed: 29800372]

16. Miller PD, Hattersley G, Riis BJ, Williams GC, Lau E, Russo LA, et al. Effect of Abaloparatide vs Placebo on New Vertebral Fractures in Postmenopausal Women With Osteoporosis: A Randomized Clinical Trial. JAMA. 2016;316(7):722–33. [PubMed: 27533157]

17. Clemens TL, Cormier S, Eichinger A, Endlich K, Fiaschi-Taesch N, Fischer E, et al. Parathyroid hormone-related protein and its receptors: nuclear functions and roles in the renal and cardiovascular systems, the placental trophoblasts and the pancreatic islets. Br J Pharmacol. 2001;134(6):1113–36. [PubMed: 11704631]

18. Hattersley G, Dean T, Corbin BA, Bahar H, Gardella TJ. Binding Selectivity of Abaloparatide for PTH-Type-1-Receptor Conformations and Effects on Downstream Signaling. Endocrinology. 2016;157(1):141–9. [PubMed: 26562265]

19. Ricarte FR, Le Henaff C, Kolupaeva VG, Gardella TJ, Partridge NC. Parathyroid hormone(1–34) and its analogs differentially modulate osteoblastic Rankl expression via PKA/SIK2/SIK3 and PP1/PP2A-CRTC3 signaling. J Biol Chem. 2018;293(52):20200–13. [PubMed: 30377251]

20. Bahar H, Gallacher K, Downall J, Nelson CA, Shomali M, Hattersley G. Six Weeks of Daily Abaloparatide Treatment Increased Vertebral and Femoral Bone Mineral Density, Microarchitecture and Strength in Ovariectomized Osteopenic Rats. Calcif Tissue Int. 2016;99(5):489–99. [PubMed: 27395059]

21. Chew CK, Clarke BL. Abaloparatide: Recombinant human PTHrP (1–34) anabolic therapy for osteoporosis. Maturitas. 2017;97:53–60. [PubMed: 28159062]

22. Varela A, Chouinard L, Lesage E, Smith SY, Hattersley G. One Year of Abaloparatide, a Selective Activator of the PTH1 Receptor, Increased Bone Formation and Bone Mass in Osteopenic Ovariectomized Rats Without Increasing Bone Resorption. J Bone Miner Res. 2017;32(1):24–33. [PubMed: 27748532]

23. Moreira CA, Fitzpatrick LA, Wang Y, Recker RR. Effects of abaloparatide-SC (BA058) on bone histology and histomorphometry: The ACTIVE phase 3 trial. Bone. 2017;97:314–9. [PubMed: 27826127]

24. Leder BZ, O'Dea LS, Zanchetta JR, Kumar P, Banks K, McKay K, et al. Effects of abaloparatide, a human parathyroid hormone-related peptide analog, on bone mineral density in postmenopausal women with osteoporosis. J Clin Endocrinol Metab. 2015;100(2):697–706. [PubMed: 25393645]

25. Makino A, Takagi H, Takahashi Y, Hase N, Sugiyama H, Yamana K, et al. Abaloparatide Exerts Bone Anabolic Effects with Less Stimulation of Bone Resorption-Related Factors: A Comparison with Teriparatide. Calcif Tissue Int. 2018;103(3):289–97. [PubMed: 29725706]

26. Varela A, Chouinard L, Lesage E, Guldberg R, Smith SY, Kostenuik PJ, et al. One year of abaloparatide, a selective peptide activator of the PTH1 receptor, increased bone mass and strength in ovariectomized rats. Bone. 2017;95:143–50. [PubMed: 27894941]

27. Doyle N, Varela A, Haile S, Guldberg R, Kostenuik PJ, Ominsky MS, et al. Abaloparatide, a novel PTH receptor agonist, increased bone mass and strength in ovariectomized cynomolgus monkeys by increasing bone formation without increasing bone resorption. Osteoporos Int. 2018;29(3):685–97. [PubMed: 29260289]

28. Chandler H, Lanske B, Varela A, Guillot M, Boyer M, Brown J, et al. Abaloparatide, a novel osteoanabolic PTHrP analog, increases cortical and trabecular bone mass and architecture in orchiectomized rats by increasing bone formation without increasing bone resorption. Bone. 2019;120:148–55. [PubMed: 30343166]

29. Bouxsein ML, Boyd SK, Christiansen BA, Guldberg RE, Jepsen KJ, Muller R. Guidelines for assessment of bone microstructure in rodents using micro-computed tomography. J Bone Miner Res. 2010;25(7):1468–86. [PubMed: 20533309]

30. Tamasi JA, Vasilov A, Shimizu E, Benton N, Johnson J, Bitel CL, et al. Monocyte chemoattractant protein-1 is a mediator of the anabolic action of parathyroid hormone on bone. J Bone Miner Res. 2013;28(9):1975–86. [PubMed: 23519994]

31. Dempster DW, Compston JE, Drezner MK, Glorieux FH, Kanis JA, Malluche H, et al. Standardized nomenclature, symbols, and units for bone histomorphometry: a 2012 update of the report of the ASBMR Histomorphometry Nomenclature Committee. J Bone Miner Res. 2013;28(1):2–17. [PubMed: 23197339]

32. Parfitt AM, Drezner MK, Glorieux FH, Kanis JA, Malluche H, Meunier PJ, et al. Bone histomorphometry: standardization of nomenclature, symbols, and units. Report of the ASBMR Histomorphometry Nomenclature Committee. J Bone Miner Res. 1987;2(6):595–610. [PubMed: 3455637]

33. Amrhein V, Greenland S, McShane B. Scientists rise up against statistical significance. Nature. 2019;567(7748):305–7. [PubMed: 30894741]

34. Glatt V, Canalis E, Stadmeyer L, Bouxsein ML. Age-related changes in trabecular architecture differ in female and male C57BL/6J mice. J Bone Miner Res. 2007;22(8):1197–207. [PubMed: 17488199]

35. Ishizuya T, Yokose S, Hori M, Noda T, Suda T, Yoshiki S, et al. Parathyroid hormone exerts disparate effects on osteoblast differentiation depending on exposure time in rat osteoblastic cells. J Clin Invest. 1997;99(12):2961–70. [PubMed: 9185520]

36. Locklin RM, Khosla S, Turner RT, Riggs BL. Mediators of the biphasic responses of bone to intermittent and continuously administered parathyroid hormone. J Cell Biochem. 2003;89(1):180–90. [PubMed: 12682918]

37. Nakagawa N, Kinosaki M, Yamaguchi K, Shima N, Yasuda H, Yano K, et al. RANK is the essential signaling receptor for osteoclast differentiation factor in osteoclastogenesis. Biochem Biophys Res Commun. 1998;253(2):395–400. [PubMed: 9878548]

38. Simonet WS, Lacey DL, Dunstan CR, Kelley M, Chang MS, Luthy R, et al. Osteoprotegerin: a novel secreted protein involved in the regulation of bone density. Cell. 1997;89(2):309–19. [PubMed: 9108485]

39. Nakatani T, Partridge NC. MEF2C Interacts With c-FOS in PTH-Stimulated Mmp13 Gene Expression in Osteoblastic Cells. Endocrinology. 2017;158(11):3778–91. [PubMed: 28973134]

40. Partridge NC, Jeffrey JJ, Ehlich LS, Teitelbaum SL, Fliszar C, Welgus HG, et al. Hormonal regulation of the production of collagenase and a collagenase inhibitor activity by rat osteogenic sarcoma cells. Endocrinology. 1987;120(5):1956–62. [PubMed: 3032574]

41. Tyson DR, Swarthout JT, Partridge NC. Increased osteoblastic c-fos expression by parathyroid hormone requires protein kinase A phosphorylation of the cyclic adenosine 3',5'-monophosphate response element-binding protein at serine 133. Endocrinology. 1999;140(3):1255–61. [PubMed: 10067851]

42. Amizuka N, Warshawsky H, Henderson JE, Goltzman D, Karaplis AC. Parathyroid hormone-related peptide-depleted mice show abnormal epiphyseal cartilage development and altered endochondral bone formation. J Cell Biol. 1994;126(6):1611–23. [PubMed: 8089190]

43. Weir EC, Philbrick WM, Amling M, Neff LA, Baron R, Broadus AE. Targeted overexpression of parathyroid hormone-related peptide in chondrocytes causes chondrodysplasia and delayed endochondral bone formation. Proc Natl Acad Sci U S A. 1996;93(19):10240–5. [PubMed: 8816783]

44. Horwitz MJ, Tedesco MB, Garcia-Ocana A, Sereika SM, Prebehala L, Bisello A, et al. Parathyroid hormone-related protein for the treatment of postmenopausal osteoporosis: defining the maximal tolerable dose. J Clin Endocrinol Metab. 2010;95(3):1279–87. [PubMed: 20061412]

45. Martin TJ. Parathyroid Hormone-Related Protein, Its Regulation of Cartilage and Bone Development, and Role in Treating Bone Diseases. Physiol Rev. 2016;96(3):831–71. [PubMed: 27142453]

46. Wysolmerski JJ. Interactions between breast, bone, and brain regulate mineral and skeletal metabolism during lactation. Ann N Y Acad Sci. 2010;1192:161–9. [PubMed: 20392232]

47. Hsu H, Lacey DL, Dunstan CR, Solovyev I, Colombero A, Timms E, et al. Tumor necrosis factor receptor family member RANK mediates osteoclast differentiation and activation induced by osteoprotegerin ligand. Proc Natl Acad Sci U S A. 1999;96(7):3540–5. [PubMed: 10097072]

48. Nakatani T, Chen T, Johnson J, Westendorf JJ, Partridge NC. The Deletion of Hdac4 in Mouse Osteoblasts Influences Both Catabolic and Anabolic Effects in Bone. J Bone Miner Res. 2018;33(7):1362–75. [PubMed: 29544022]

49. Keller H, Kneissel M. SOST is a target gene for PTH in bone. Bone. 2005;37(2):148–58. [PubMed: 15946907]

50. Kramer I, Halleux C, Keller H, Pegurri M, Gooi JH, Weber PB, et al. Osteocyte Wnt/beta-catenin signaling is required for normal bone homeostasis. Mol Cell Biol. 2010;30(12):3071–85. [PubMed: 20404086]

51. Kramer I, Loots GG, Studer A, Keller H, Kneissel M. Parathyroid hormone (PTH)-induced bone gain is blunted in SOST overexpressing and deficient mice. J Bone Miner Res. 2010;25(2):178–89. [PubMed: 19594304]

52. Cosman F, Hattersley G, Hu MY, Williams GC, Fitzpatrick LA, Black DM. Effects of Abaloparatide-SC on Fractures and Bone Mineral Density in Subgroups of Postmenopausal Women With Osteoporosis and Varying Baseline Risk Factors. J Bone Miner Res. 2017;32(1):17–23. [PubMed: 27612281]

53. Seeman E, Delmas PD. Reconstructing the skeleton with intermittent parathyroid hormone. Trends Endocrinol Metab. 2001;12(7):281–3. [PubMed: 11504661]

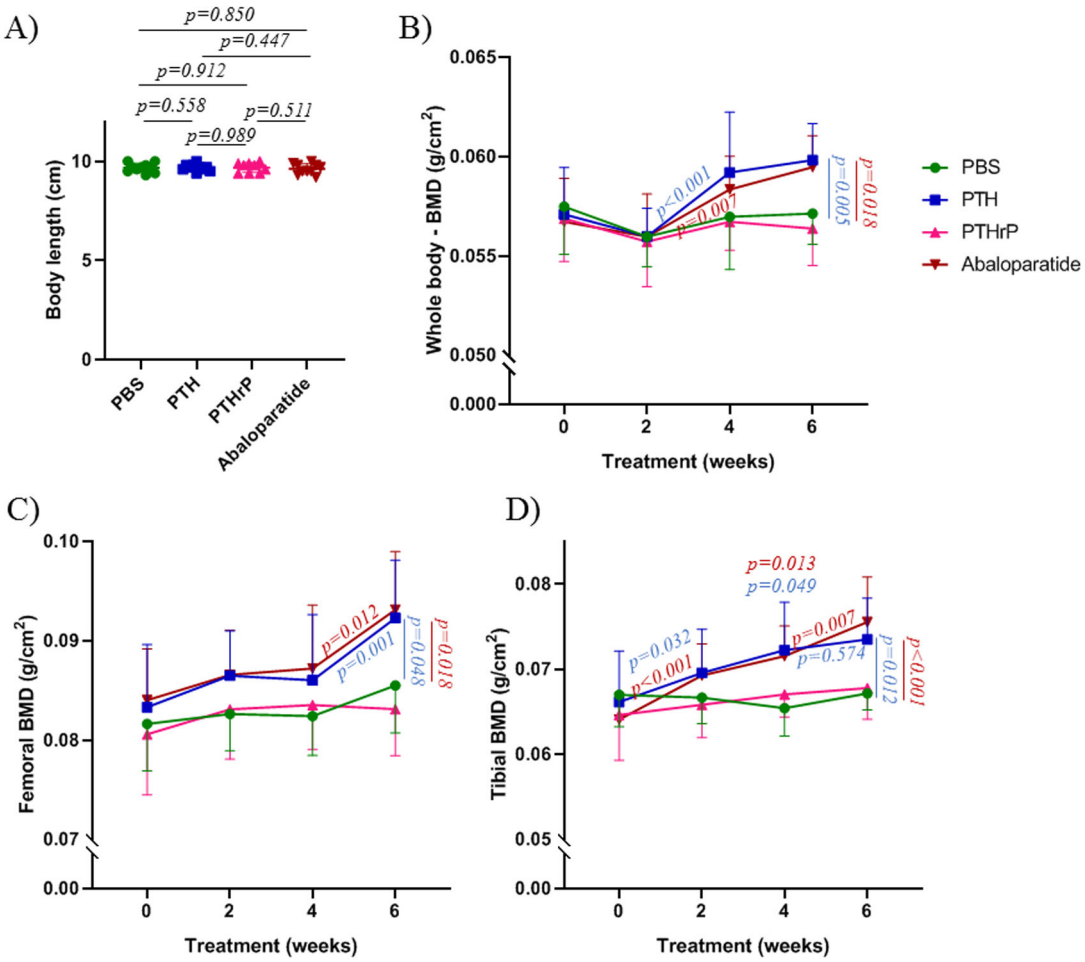

Figure 1: PTH (1-34) and abaloparatide improved bone mineral density whereas PTHrP (1-36) had no effect in mice

A) Mouse body length at the end of the treatments. B-D) Throughout the course of the study, DEXA-Piximus was performed every 2 weeks to measure bone mineral density (BMD) of B) whole body, C) femur and D) tibia. Ten mice per group. Results are means ± SD. All data were analyzed for normality and equivalence of variance before a 2 way ANOVA – repeated measures followed by Bonferroni's multiple comparison test. All exact *p* values are indicated in Fig. 1A. In Figs. 1B-D, the *p* values at one time point compare the peptides to the vehicle controls. The *p* values on the lines compare one peptide at the two connected time points.

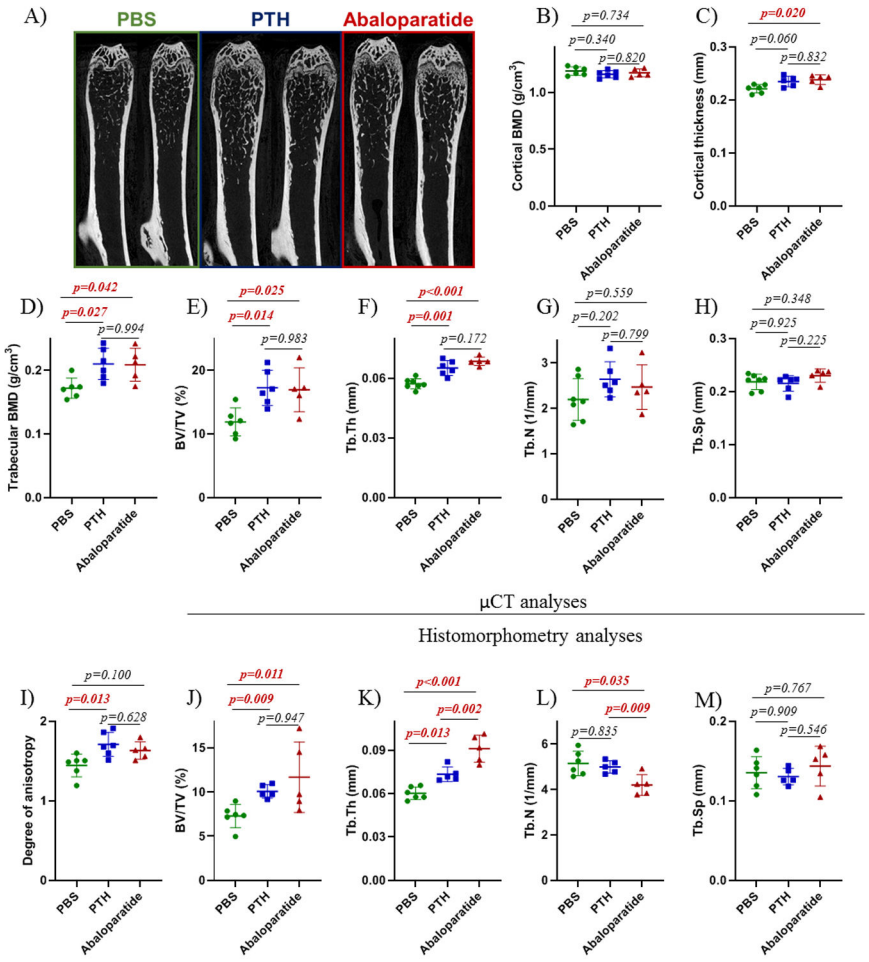

Figure 2: PTH (1-34) and abaloparatide similarly improved trabecular bone volume and cortical thickness in mice

A) Representative images of right femur showing the changes in trabecular bone in male mice treated with PTH (1-34) or abaloparatide at 4 months of age for 6 weeks. Femurs were prepared for high resolution µCT and images were reconstructed with NRecon software. B - C) A 600 µm cortical volume corresponding to 62 slices of the mid-diaphysis was examined for B) cortical bone mineral density and C) cortical thickness. D - I) A 970 µm volume corresponding to 100 slices of the mid-metaphysis was examined for trabecular bone microarchitecture. D) trabecular bone mineral density (BMD), E) trabecular bone volume (BV/TV), F) trabecular thickness (Tb.Th), G) trabecular number (Tb.N), H) trabecular separation (Tb.Sp) and I) degree of anisotropy. J – M) Femoral thin sections (5 µm) were stained with Masson's trichrome. Measurements were conducted in the secondary spongiosae for histomorphometric analysis of J) trabecular bone volume (BV/TV), K) thickness of trabeculae (Tb.Th), L) number of trabeculae (Tb.N) and M) space between trabeculae (Tb.Sp). 5-7 mice per group, results are means ± SD. All data were analyzed for normality and equivalence of variance before a 1 way ANOVA followed by a Tukey's multiple comparison test. The histomorphometric analysis of bone volume did not show equivalence of variance so we used Kruskal-Wallis, a non-parametric test. All exact *p* values are shown.

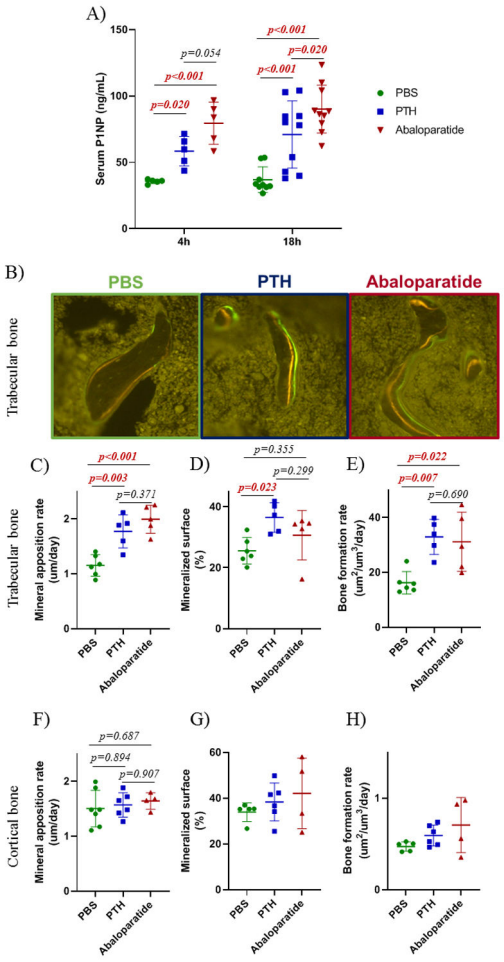

Figure 3: PTH (1-34) and abaloparatide similarly improved bone formation in mice

At the end of the treatments, sera were collected at 4 or 18 h after the last injection. A) To analyze bone formation, serum P1NP levels were measured by ELISA in male mice treated with PTH (1-34) or abaloparatide. B - D) Mice were injected with tetracycline at day 7 and with calcein at day 2 before death to determine bone formation. Femoral thin sections (10 μm) were obtained. B) Representative images of right femurs showing differences in double labeling in trabecular bone in mice treated with PTH (1-34) or abaloparatide. Measurements were performed in the secondary spongiosae for trabecular dynamic analyses: C) mineral apposition rate, D) mineralized surface and E) bone formation rate. Measurements were performed in the mid-diaphysis for cortical dynamic analyses: F) cortical mineral apposition rate, G) cortical mineralized surface and H) cortical bone formation rate. 5-7 mice per group, results are means ± SD. Histomorphometric data were analyzed for normality and equivalence of variance before a 1 way ANOVA followed by a Tukey's multiple comparison test. The bone formation rate (cortical and trabecular bone) and the cortical mineralized surface did not show equivalence of variance so we used Kruskal-Wallis, a non-parametric test. For the serum P1NP, normal distribution was not demonstrated so a rank transformation was done before performing new normality and equivalence of variance tests and 2 way ANOVA followed by Bonferroni's multiple comparison test. Most exact *p* values are shown.

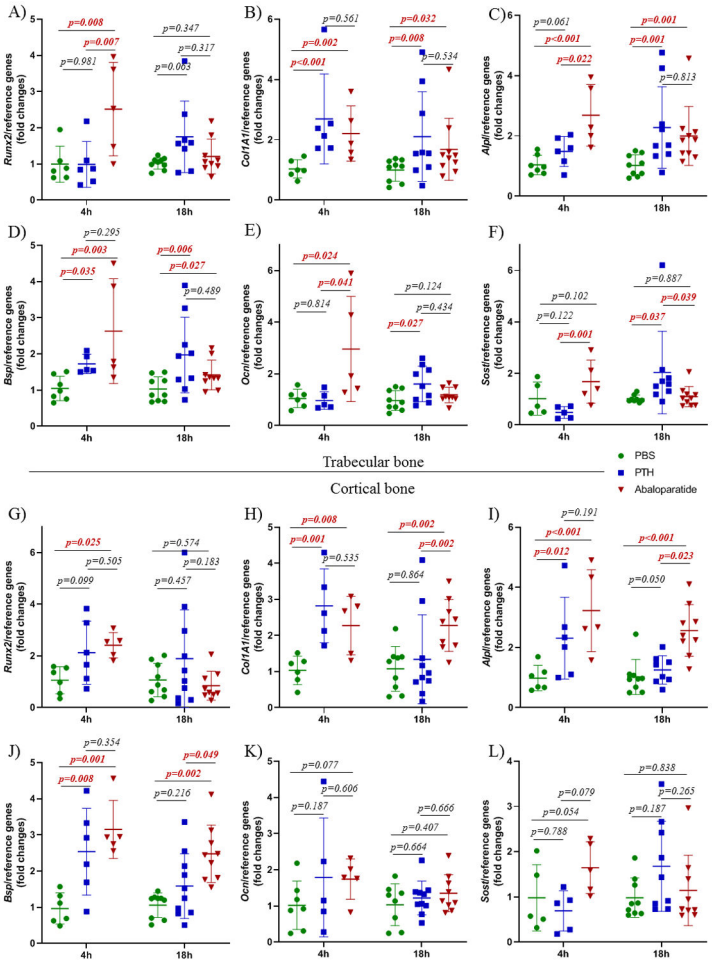

Figure 4: PTH (1-34) and abaloparatide differentially regulated osteoblastic gene expression.

A - F) Osteoblastic gene expression was measured at 4 h and 18 h after the last injections. A-F: Trabecular-rich tibial bone: A) *Runx2*, B) *Col1A1*, C) *Alpl*, D) Bone sialoprotein or *Bsp*, E) *Ocn*, F) *Sost*. G - L) Osteocyte-rich cortical tibial bone: G) *Runx2*, H) *Col1A1*, I) *Alpl*, J) *Bsp*, K) *Ocn*, L) *Sost*. 5-10 mice per group, results are means ± SD. For these data, normal distribution was not demonstrated so a rank transformation was done before performing new normality and equivalence of variance tests and 2 way ANOVA followed by Bonferroni's multiple comparison test. For trabecular *Sost* and cortical *Bsp* and *Runx2*, we had to use the non-parametric Kruskal-Wallis test. All exact *p* values are shown.

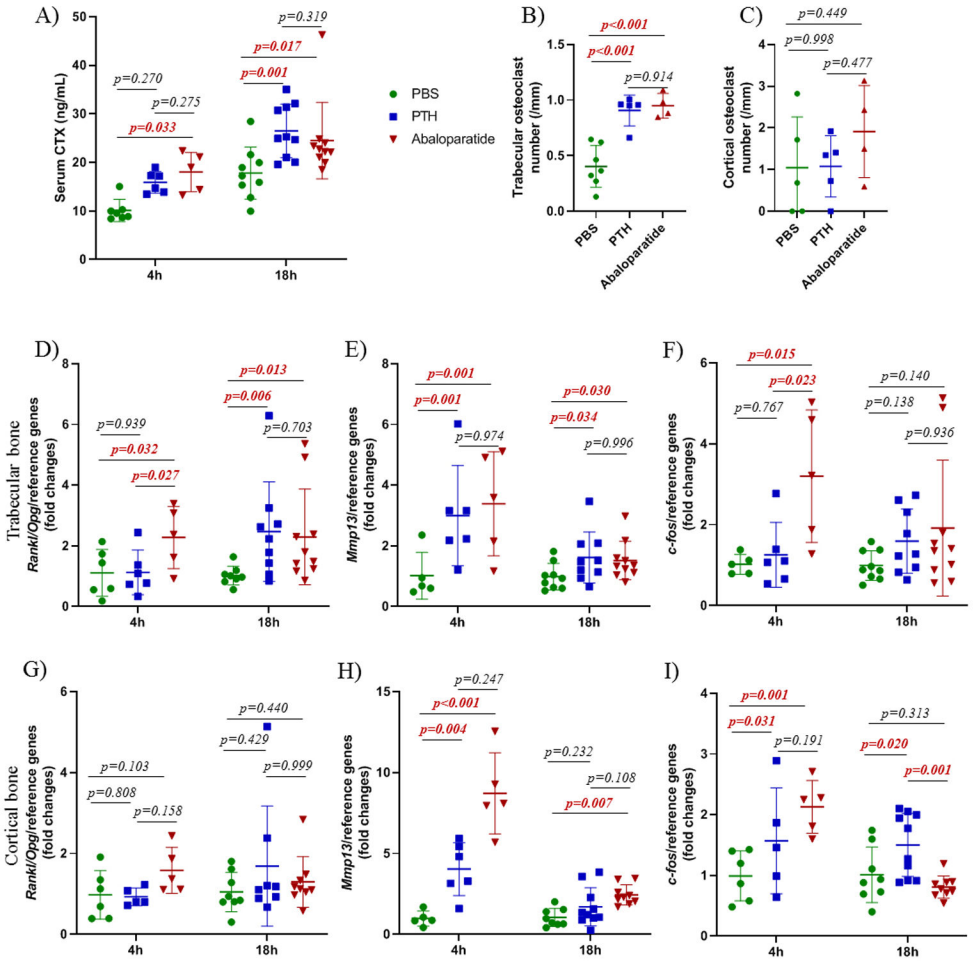

Figure 5: Both PTH (1-34) and abaloparatide increased bone resorption in mice

At the end of the treatments, mice were killed at 4 or 18 h after the last injections. To assess bone resorption, A) serum CTX levels were measured by ELISA in male mice treated with PTH (1-34) or abaloparatide. B-C) Femurs were fixed in 70% ethanol, dehydrated and embedded in methacrylate. TRAP staining was done in order to count osteoclasts on bone surfaces, B) in trabecular area and, C) in cortical bone in the mid-diaphysis. Two tibiae from each animal were divided into subcortical trabecular-rich bone, bone marrow and cortical bone (osteocyte-rich bone). Total RNA was isolated and qRT-PCR was performed. Catabolic gene expression was measured in the trabecular-rich fraction for D) *Rankl*/*Opg* ratio, E) *Mmp13*, F) *c-fos* and in cortical bone for G) *Rankl*/*Opg* ratio, H) *Mmp13*, I) *c-fos*. Expression of all genes was compared with housekeeping genes and shown as fold change compared with control animals. 5-10 mice per group, results are means ± SD. All data were analyzed for normality and equivalence of variance. For histomorphometry analyses, we used a 1 way ANOVA followed by Tukey's multiple comparison test. For the qPCR and CTX analyses, normal distribution was not achieved so rank transformation was performed before new normality and equivalence of variance tests were done and 2 way ANOVA followed by Bonferroni's multiple comparison test was then conducted. All exact *p* values are shown.